Kinetics of Phase Separation in $Mn_{0.67}Cu_{0.33}$

B. D. Gaulin and S. Spooner
Solid State Division, Oak Ridge National Laboratory, Oak Ridge, Tennessee 37831

and

Y. Morii
Physics Division, Japan Atomic Energy Research Institute, Tokai, Ibaraki 391-11, Japan
(Received 9 March 1987)

We have examined the kinetics of phase separation in $Mn_{0.67}Cu_{0.33}$ using time-resolved neutron-scattering techniques. In an early-time regime, the kinetics follows the Cahn-Hilliard-Cook linear theory of spinodal decomposition. There is an intermediate stage. Then, at a late time, dynamic scaling is obeyed. The time dependence of the wave vector at maximum scattering intensity (which is inversely proportional to the average linear domain size) can be well described over the entire late-time regime and much of the intermediate-time regime by arguments recently put forward for earlier-time corrections to the limitingly late-time stages of phase separation.

PACS numbers: 64.75.+g, 61.50.Ks, 81.40.Cd

The kinetics of first-order phase transitions[1] has been of prime interest because of its technological importance in materials science. More recently, the physics community has turned its attention to this field as part of a wider effort examining nonequilibrium phenomena, growth processes, and pattern formation. Most of this effort has been in theoretical or computer-simulation studies of systems which undergo either phase-separation (in which the order parameter is conserved) or order-disorder (in which the order parameter is not conserved) transitions. Only a few systems have been examined experimentally with techniques capable of measuring appropriate time dependence of spatial correlations. All of these studies have considered how a quenched system evolves towards an equilibrium state below an ordering temperature.

Understanding in this field is in transition. Two ideas are significant in the understanding of phase-transition kinetics. First, spatial self-similarity and dynamic scaling are expected to describe the evolution of the structure at late times. A single length, the average linear domain size, would characterize the decomposing structure and the pattern of the structure at different times differs only in its scale. Second, the growth rate of the characteristic length at late times is believed to follow an asymptotic late-time dependence. However, conflicting predictions have recently been put forward[2,3] concerning the form of this dependence.

Experimental studies on phase-separating systems have examined metal alloys,[4] glasses,[5] liquids,[6] and polymer blends.[7] However, a definitive determination of the time-dependent phase-separation behavior has not been made.[8] We have undertaken a time-resolved small-angle neutron-scattering (SANS) study of $Mn_{0.67}Cu_{0.33}$ to examine the kinetics of phase separation over early and late times with the purpose of establishing a comprehensive experimental description of the process.

The Cu-Mn alloy system is known to have a miscibility gap[9] in Mn-rich alloys. The variation of solid-solution lattice parameters[10] in the range of phase-separation composition is small, which leads to a minimal strain-energy effect. Copper and manganese possess neutron-scattering lengths of opposite sign [$b_{(Mn)}/b_{(Cu)} = -0.48$]. Consequently, at zero wave-vector transfer, $Mn_{0.67}Cu_{0.33}$ shows approximately zero coherent scattering intensity. What is more, a disordered $Mn_{0.67}Cu_{0.33}$ sample displays approximately zero coherent neutron scattering at all wave-vector transfers. Thus, this composition represents an experimental system where the coherent, intrinsic background scattering from the sample is kept to an absolute minimum. The $Mn_{0.67}Cu_{0.33}$ alloy lies near the center of the miscibility gap and at 450 °C the decomposition observation point is well within the classical spinodal instability regime.

The experiments were carried out on the 30-m small-angle scattering machine of the National Center for Small-Angle Scattering Research at the Oak Ridge National Laboratory. Three sample-to-detector distances were employed in order to follow the time development of the structure function over a long time. Counting times were 30 sec at 2.14 m, 300 sec at 4.73 m, and 420 sec at 12.75 m. The wavelength was 4.75 Å. The high-purity polycrystalline sample was mounted in a specially designed rapid-quench furnace.[11] The sample was solution treated at 800 °C for at least 45 min before quenching. The phase-separation boundary for this alloy is 560 °C. Scattering-data collection was started before the quench to 450 °C, and temperature control was established in 30 sec. Data sets were stored at the above-mentioned time intervals in the course of decomposition.

The structure function, $S(Q)$, of the SANS experiment directly measures the equal-time concentration correlation function. It displays a peaked form and the wave vector, Q_{max}, at which $S(Q)$ is a maximum occurs

such that, on average, the scattering lengths within each domain add up in phase. Therefore, Q_{max} is inversely proportional to the average domain size.

The measured intensity was corrected for detector sensitivity and background, where the background was taken to be the scattering measured at 800 °C. $S(Q)$ was thus determined for times from 65 to 21 109 sec. These data were then reduced to one-dimensional data sets by circular averaging of the radially symmetric data. Each of these data sets was fitted by a general form for the purpose of determining $Q_{max}(t)$. The excellent fits yielded values of $Q_{max}(t)$ which can be extracted from Fig. 1.

The linear theory of phase separation due to Cahn and Hilliard[12] was extended to include thermal fluctuations in the final quenched state by Cook.[13] The theories make a sharp distinction between unstable states (which evolve via spinodal decomposition) and metastable states (which evolve via nucleation and growth). For spinodal decomposition, the Cahn-Hilliard-Cook (CHC) structure function is

$$S(Q,t)=\tilde{S}(Q)\exp[RQ^2(Q_c^2-Q^2)t]-[\alpha T/(Q_c^2-Q^2)]\{1-\exp[RQ^2(Q_c^2-Q^2)t]\},$$

where T is the final-state temperature, and R is related to the mobility of the system in the final state, as well as the position of this state on the phase diagram. Consequently, the function $\tilde{S}(Q)$ is amplified exponentially for wave vectors below some critical wave vector, Q_c, while the maximum amplification is at the time-independent value of $Q_c/\sqrt{2}$.

Figure 2 shows our early-time data for times from 65 to 597 sec. With use of an assumed form of $\tilde{S}(Q)$, our early-time data could be very well represented by the CHC structure factor. The form of $\tilde{S}(Q)$ used to propagate the time-evolving structure functions is shown at the bottom of Fig. 2 and has been divided by 2 for clarity of presentation. Our best description of these data used $Q_c=0.139$ Å^{-1}, $R=32$ Å^4/sec, and $\alpha T=2.8$ in units of $\tilde{S}(Q)$ Å^{-2}. The solid lines through the data show the excellent description of our data by the theory for times less than 300 sec. For greater times, the description becomes systematically worse as can be seen in the upper panel of Fig. 2. It is clear that for these larger times, the peak in the measured $S(Q,t)$ moves to lower wave vectors with time, while the peak intensity lags progressively farther behind its predicted value. This failure of the

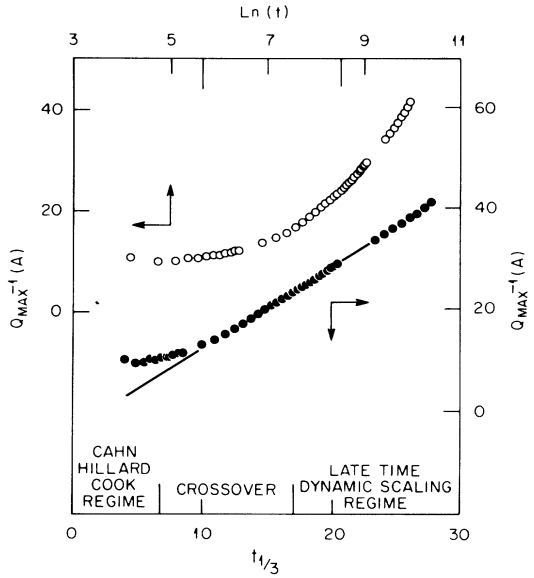

FIG. 1. Q_{max}^{-1} as a function of (time)$^{1/3}$ and the logarithm of time (with time in seconds) for $Mn_{0.67}Cu_{0.33}$. The solid line is the fit of Huse's form of $Q_{max}(t)$ to our data, as discussed in the text. The longer lines on the upper y axis denote the same boundaries of the early-, intermediate-, and late-time regimes shown on the lower y axis.

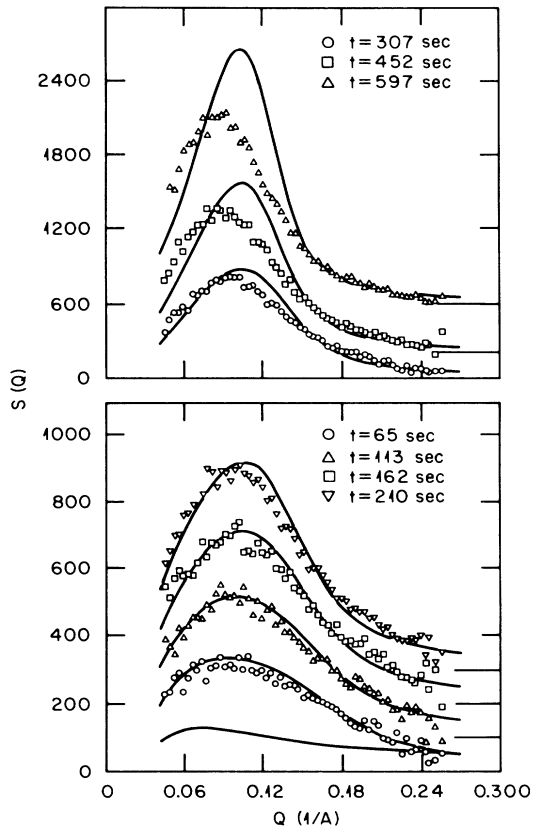

FIG. 2. The $S(Q,t)$ data sets at relatively early times. The solid lines are the results of the fit of the CHC theory [with the $\frac{1}{2}\tilde{S}(Q)$ base function shown at the bottom of the figure] to the data. Systematic discrepancies are clear for times longer than 300 sec. Data sets have zero $S(Q)$ values shown by the solid lines to the right of the panels for clarity of presentation.

CHC theory at later times is due to nonlinearity in the decomposition process which is not included in the theory. Recently, Carmesin, Heerman, and Binder[14] have argued that features of CHC theory can be induced by the effects of finite quench rate. To examine this point we performed a quench from 800 °C, first to 575 °C, where we waited for 30 sec before quenching further to 450 °C. This different cooling history resulted in a relatively weak distribution of the scattering characteristic of the structure at 575 °C in addition to the peak scattering obtained by a direct quench. Subtraction of the scattering characteristic of 575 °C left a scattering pattern that was essentially identical to that obtained by direct quenching. It was thus demonstrated that quenching effects did not exert an important influence in the early scattering patterns. Thus, to the best of our knowledge, this is the first demonstration of the applicability of the CHC theory over any time regime for a system with non-long-range interactions (excluding polymer blends).

Binder,[15] as well as Grant *et al.*,[16] has shown that the maximum time over which the CHC theory would apply is related to the range of the interactions in the system. Specifically, $t_{\max} \simeq \ln L$, where L is the range of the interactions.

A dimensionless relative range-of-interaction parameter L can be extracted with use of our measured $t_{\max}$ value, following the arguments set out by Grant *et al.*[16] We obtain $L \simeq 3.0$ which should be compared with $L = 1$ for the nearest-neighbor Ising model, and $L \simeq 20$ for a typical polymer blend with a chain length of 400 monomer units. We conclude that the interaction between the atoms in $Mn_{0.67}Cu_{0.33}$ is of intermediate range, which might be expected for a metal alloy.

At late times a dynamic scaling of the time-dependent structure is predicted. The expected form of the structure function is

$$S(Q,t) = [Q_{\max}(t)]^{-d} F(Q/Q_{\max}(t)),$$

where d is the dimensionality of the system, while $F(Q/Q_{\max}(t))$ is the universal scaling function. The validity of this dynamic scaling is usually checked by examining the time dependence of $S(Q_{\max})$ and $Q_{\max}(t)$. If $Q_{\max} \propto t^{-a}$, then $S(Q_{\max}(t)) \propto t^{da}$ if this scaling is obeyed. Although several systems have shown this behavior, others have not, and a consistent experimental picture does not exist.[17]

Figure 3 shows our results for $(Q_{\max})^3 S(Q)$, the expected form of the scaling function $F(Q/Q_{\max}(t))$, at later time. Data sets of $F(Q/Q_{\max}(t))$ for times from 5115 through 8429 sec are shown in the top panel of Fig. 3. These data sets fall almost precisely on top of one another, as do later-time data sets from 12582 through 21109 sec (which are not shown in Fig. 3 as the absolute intensities at the 4.73- and 12.75-m sample-detector distance settings are not normalized to each other). This

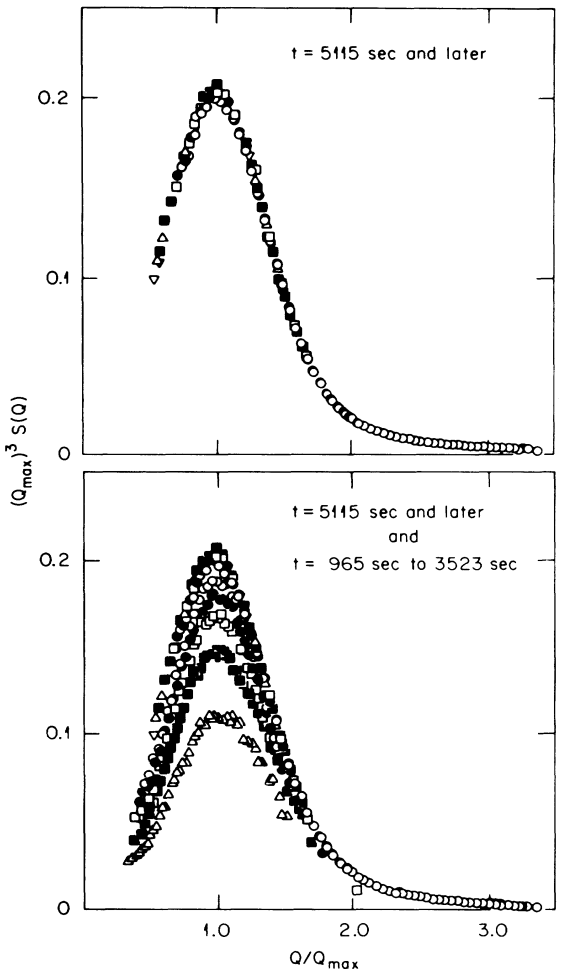

FIG. 3. Top: Scaling behavior of the data sets of $F(Q/Q_{\max}) = Q_{\max}^3 S(Q)$ for times exceeding 5000 sec. Bottom: Same data sets as the top panel, as well as five data sets at 965, 1602, 2239, 2886, and 3523 sec. These earlier-time data sets depart from the scaling relation to a systematically greater extent with decreasing time.

indicates that at these late times, the dynamic scaling relation is followed exactly within the limits of the experimental error bars of the data. At earlier times, the data sets follow the scaling form to a systematically lesser and lesser extent, as can be seen in the bottom panel of Fig. 3. Hence, we can explicitly see the breakdown of the late-time scaling for times less than 5000 sec.

Of course, given that at early time CHC theory is obeyed, the late-time dynamic scaling must fail at some point as CHC theory does not exhibit this scaling. We consequently divide the kinetic behavior into three regimes: an early-time regime where CHC theory applies, a late-time regime where dynamic scaling applies, and a crossover stage connecting the early- and late-time regimes. These regimes are shown in Fig. 1 for $Mn_{0.67}Cu_{0.33}$. Dynamic scaling would be obscured if a

significant part of the test data were in the crossover regime. We believe that this is the cause of inconsistent experimental findings on late-time dynamic scaling.

The time dependence of the average linear domain size, $R(t)$, is currently a controversial theoretical point. As $Q_{\max}(t) \simeq 1/R(t)$, the relevant arguments can be tested experimentally. Lifshitz and Slyozov[18] originally argued $R(t) \simeq t^{1/3}$ at late times for a system which initially evolves via nucleation and growth. Very recently, Huse[2] has argued for the same result for a system which initially evolves via spinodal decomposition; however, he has also produced earlier-time corrections to this behavior based on the existence of an enhanced interfacial atomic conductivity. This correction produces the relation

$$Q_{\max}^{-1} \sim R(t) = At^{1/3} + R_0,$$

where R_0 is a microscopic length. The competing argument,[3] a zero-temperature renormalization-group approach, predicts $R(t) \sim \ln t$ and is valid only at late times.

Our data for $Q_{\max}^{-1}$ versus time is plotted in Fig. 1 in such a way as to test these two dependencies. A logarithmic time dependence is not observed over any convincing time range. An excellent fit can be made to our data over all the late-time scaling regime and most of the crossover regime with use of the form proposed by Huse, and this is shown as the solid line in Fig. 1. However, the intercept at $t = 0$, which is proportional to R_0, is negative. This argument is a correction to late-time behavior and not an early-time argument; thus it is not surprising that it does not describe the early-time CHC regime. If we regard this relation as being valid only for times exceeding the $t_{\max} = 300$ sec region of validity of the CHC theory, then the microscopic length of interest is $R_0' = R(t_{\max})$. This value is positive [being $R_0' \sim \pi/Q_{\max}(t_{\max})$ which is $\simeq 23$ Å or 6 lattice spacings] as well as considerably smaller than the average domain size in the system at any time, and therefore microscopic. If the late-time data are fitted by a straight power-law dependence, the fit exponent is -0.37 ± 0.03.

In conclusion, the kinetics of phase separation in $Mn_{0.67}Cu_{0.33}$ displays three time regimes. In the early-time regime, the scattering is described by CHC theory. There is a crossover stage. In the late-time regime, dynamic scaling applies. Arguments based on Huse's work permit us to describe the $Q_{\max}(t)$ behavior over all of the late-time scaling regime and most of the crossover regime. In addition to demonstrating a consistent description of decomposition over a wide kinetic range, these findings underscore the importance of extending theoretical development from limitingly long times to earlier times.

This work has benefitted from useful discussions with M. Grant and M. Hagen. Research was carried out under the U.S.-Japan Cooperative Program on Neutron Scattering, and was supported by the U.S. Department of Energy under Contract No. DE-AC05-84OR21400 with Martin Marietta Energy Systems, Inc., and by the National Science Foundation under Grant No. DMR 7724459. One of us (B.D.G.) is the holder of a National Science and Engineering Research Council of Canada postdoctoral fellowship.

[1]J. D. Gunton, M. San Miguel, and P. S. Sahni, in *Phase Transition and Critical Phenomena,* edited by C. Domb and J. L. Lebowitz (Academic, London, 1983), Vol. 8.

[2]D. A. Huse, Phys. Rev. B **74**, 7845 (1986).

[3]G. F. Mazenko, O. T. Valls, and F. C. Zhang, Phys. Rev. B **31**, 4453 (1985), and **32**, 5807 (1985); O. T. Valls and G. F. Mazenko, to be published.

[4]For example, S. Katano and M. Iizumi, Phys. Rev. Lett. **52**, 835 (1984); S. Komura, K. Osamura, H. Fujii, and T. Takeda, Phys. Rev. B **30**, 2944 (1984).

[5]A. F. Craievich, J. M. Sanchez, and C. E. Williams, Phys. Rev. B **34**, 2762 (1986).

[6]M. Takahashi, H. Horiuchi, S. Kinoshita, Y. Ohyama, and T. Nose, J. Phys. Soc. Jpn. **55**, 2687 (1986).

[7]H. L. Snyder, P. Meakin, and S. Reich, J. Chem. Phys. **78**, 3334 (1983).

[8]Some of the experimental inconsistencies are discussed in H. L. Snyder and P. Meakin, J. Chem. Phys. **79**, 5588 (1983).

[9]J. M. Vitek and H. Warlimont, Met. Sci. **10**, 7 (1976).

[10]N. Cowlam, Met. Sci. **12**, 483 (1978).

[11]S. Katano, H. Motohashi, and M. Iizumi, Rev. Sci. Instrum. **57**, 1409 (1986).

[12]References 4–6 investigate this point and provide both examples and counterexamples of this behavior.

[13]H. E. Cook, Acta. Metall. **18**, 297 (1970).

[14]H. O. Carmesin, D. W. Heerman, and K. Binder, to be published.

[15]K. Binder, Phys. Rev. A **29**, 342 (1984).

[16]M. Grant, M. San Miguel, J. Viñals, and J. D. Gunton, Phys. Rev. B **31**, 3027 (1985).

[17]J. W. Cahn and J. E. Hilliard, J. Chem. Phys. **28**, 258 (1958).

[18]I. M. Lifshitz and V. V. Slyozov, J. Phys. Chem. Solids **19**, 35 (1961).